Journal of Marine Research, 72, 95–104, 2014

The relation between unstable shear layer thicknesses and turbulence lengthscales

by Eric Kunze[1]

ABSTRACT

This note explores the connection between the (i) lengthscales of unstable finescale shear layers which are responsible for turbulence production, (ii) turbulence patch thicknesses and (iii) the outer scales of turbulence, that is, the density overturn (Thorpe) and Ozmidov lengthscales, in the stratified ocean interior. Explanations are offered both for why (i) turbulence patches are often observed to be much thicker than outer turbulence scales and (ii) there is a spectral gap between finescale internal waves and the outer scales of turbulence. A finescale parameterization based on unstable shear predicts Ozmidov lengthscales smaller than unstable-shear-layer thicknesses for moderately unstable gradient Froude numbers $|V_z|/N < 5.5$ [or equivalently, gradient Richardson numbers $\mathrm{Ri} = N^2/V_z^2 > 0.03$ where $|V_z|$ is the instantaneous finescale vertical shear magnitude and N the instantaneous buoyancy frequency] for a critical gradient Froude number $\delta_c = 2$; this is little changed for critical gradient Froude numbers as low as 1. Thus, assuming that patch thicknesses correspond to unstable shear-layer thicknesses, outer turbulence lengthscales will be smaller than patch thicknesses for moderately unstable shear but not strongly unstable shear. A spectral gap between internal wave and turbulent shear arises for similar reasons.

1. Introduction

Turbulent mixing is important for a wide range of ocean phenomena – (i) driving the upwelling limb of the meridional thermohaline overturning circulation, (ii) maintaining abyssal density stratification, (iii) removing water-mass and tracer variability, and (iv) facilitating nutrient and dissolved-gas exchange between the stratified interior and surface boundary layer. Turbulence in the stratified ocean interior away from surface or bottom boundaries arises mostly from breaking internal gravity waves, most often due to instability of finescale near-inertial shear (Gregg et al., 1986; Itsweire et al., 1989; Peters et al., 1995; Polzin, 1996). However, turbulent patches are often observed to be much thicker than outer turbulence lengthscales (for example, see Gregg et al., 1986) and there is a spectral gap between the smallest internal-wave and largest turbulence lengthscales (Fig. 1; Gargett et al.,

1. Applied Physics Lab, University of Washington, 1013 NE 40th, Seattle, WA 98105-6698. ***e-mail: kunze@apl.washington.edu***

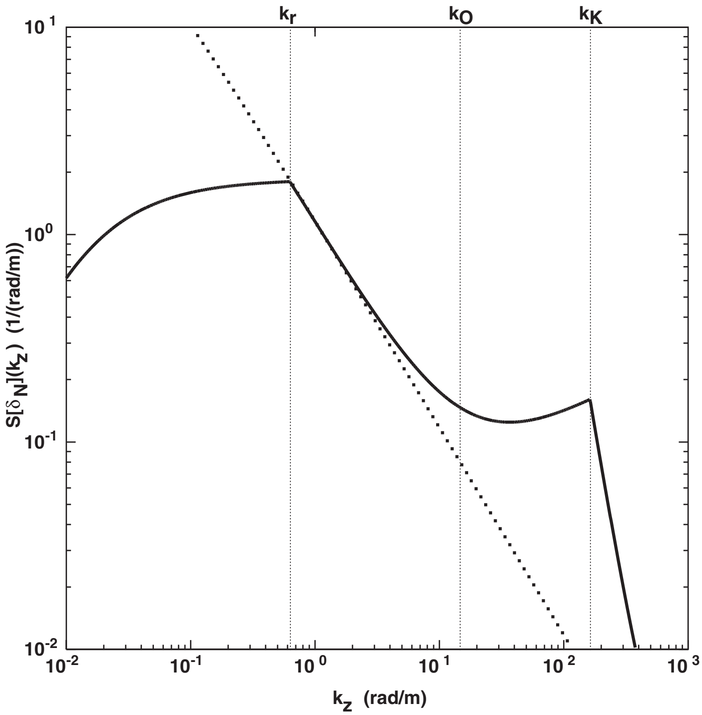

Figure 1. Vertical wavenumber k_z spectrum of gradient Froude number $\delta_N = |V_z|/N$ spanning the weakly blue Garrett-Munk internal-wave spectrum [$k_z < k_r = 2\pi/(10$ m)], the saturated k_z^{-1} spectrum [$k_r < k_z < k_O = (N^3/\varepsilon)^{1/2}$] and the Kolmogorov turbulence $k_z^{1/3}$ spectrum [$k_O < k_z < k_K = (\varepsilon/\nu^3)^{1/4}$]. This figure uses the GM76 model vertical wavenumber spectrum (Gregg and Kunze, 1991) and the dissipation rate $<\varepsilon> = 7 \times 10^{-10}$ W kg^{-1} predicted for GM-level internal waves by the Gregg-Henyey parameterization (Gregg et al., 2003) for a buoyancy frequency $N = 5.3 \times 10^{-3}$ rad s^{-1} and the GM model spectral level $E_{GM} = 6.3 \times 10^{-5}$. Sharp corners at rolloff $k_z = k_r$ and Kolmogorov k_K wavenumbers are not observed. The dotted diagonal corresponds to k_z^{-1}.

1981; Gregg et al., 1993). This note offers a dynamical explanation for these lengthscale separations though likely not the only one.

The vertical wavenumber spectrum for vertical shear (Fig. 1) is dominated by internal gravity waves for vertical wavelengths λ_z longer than a rolloff wavelength $\lambda_r \sim 10$ m; in this paper, vertical wavelengths λ_z, vertical wavenumbers $k_z = 2\pi/\lambda_z$ in rad m^{-1}, and lengthscales $L = k_z^{-1} = \lambda_z/2\pi$ will be used interchangeably. The spectrum is blue at low wavenumbers becoming approximately flat just below k_r. At higher wavenumbers $k_z > k_r$, the shear spectrum rolls off as k_z^{-1} in what is known as the saturated spectrum in the atmospheric literature (Smith et al., 1987). The rolloff wavenumber is thought to scale as E^{-1} where E is the internal-wave spectral level at lower wavenumbers, that is, $k_{GM}/k_r = E/E_{GM}$ (Gargett et al., 1981; Gregg et al., 1993; Fritts, 1984) where the GM subscript denotes the value for the canonical Garrett-and-Munk model spectrum, $E_{GM} = 6.3 \times 10^{-5}$ and $k_{GM} = 2\pi/(10 \text{ m})$ (Munk, 1981). The change in slope associated with the saturated spectrum has been explained as strongly nonlinear internal-wave interactions (Hines 1993; 1996) but it has also been suggested that it represents entirely different physics, that is, potential vorticity finestructure left behind by turbulent mixing (Polzin et al., 2003; Lelong et al., 2002; Sundermeyer and Lelong, 2005). However, it may simply represent a spectral gap between internal waves and turbulence, the k_z^{-1} slope a purely kinematic consequence of vertical straining of superimposed internal waves by other internal waves (Eckermann, 1999). At higher wavenumbers still, turbulent shear dominates between the Ozmidov wavenumber $k_O \sim (N^3/\varepsilon)^{1/2} \sim (\gamma N/K)^{1/2}$ (Osborn, 1980), where the buoyancy frequency N inhibits density overturns associated with turbulent kinetic energy dissipation rates ε, and the Kolmogorov wavenumber $k_K \sim \varepsilon/\nu^3)^{1/4}$, where molecular viscosity ν strongly damps out smaller-scale shear variance. Here, K is the turbulent diapycnal diffusivity and γ the mixing efficiency. Dimensional scaling implies a $k_z^{1/3}$ spectrum for $k_O < k_z < k_K$. The internal-wave spectrum is more or less universal while turbulence is intermittently present 5–10% of space-time (Gregg and Sanford, 1988) as are unstable shear conditions (Kunze et al., 1990; Peters et al., 1995; Polzin, 1996). A spectral description (Fig. 1) cannot capture the physics of turbulence production because it smears over these sporadic unstable shear events.

2. Shear instability

Turbulence in the ocean is neither homogeneous nor stationary, arising sporadically in most of the stratified interior. Shear instabilities, such as Kelvin-Helmholtz billows, raise heavy water above light on the largest turbulent lengthscales $L_T \sim L_O$ to produce a negative buoyancy-flux $< w'b' >$ (Fig. 2), that is, in the sense of mixing. Secondary 3-D instability then breaks down the resulting unstable density overturn (D'Asaro et al., 2004; Smyth and Moum, 2000). Anomalous density parcels rise and sink toward their original isopycnal surfaces in a positive buoyancy-flux counter to the sense of mixing. This restoration to the unperturbed stratification is partially short-circuited by molecular diffusion, resulting in net mixing. In observations, the density overturn (Thorpe) scale L_T is related to the Ozmidov lengthscale $L_O \sim 0.8 L_T$ on average (Dillon, 1982; Dillon and Park, 1987) though, as evident from Figure 2, their ratio evolves over the lifecycle of a turbulent event, with $L_T >> L_O$ during the initial overturn when turbulent dissipation rates ε are small and $L_T < L_O$ when the dissipation rate can no longer support density overturns ($\varepsilon <\sim 200\ \nu N^2$) (Gargett et al., 1984; Wijesekera and Dillon, 1997; Smyth and Moum, 2000).

A shear instability criterion can be posed in terms of gradient Froude number $\delta_N = |V_z|/N > \delta_c$ [equivalent to a gradient Richardson (1920) number criterion $\text{Ri} = N^2/V_z^2 = \delta_N^{-2} < \delta_c^{-2}$], where $|V_z| = (u_z^2 + v_z^2)^{1/2}$ is the vertical shear magnitude. A critical gradient

Figure 2. Evolution of a shear instability showing the growth of a density overturn, its breakdown into turbulence and subsequent decay along the top. Subsequent levels show the corresponding production $<u'w'>\partial U/\partial z$, buoyancy-flux $<w'b'>$, dissipation rate $\varepsilon \sim L_O^2 N^3$, change in fluctuating available potential energy APE' $= L_T^2 N^2/2$ and change in background potential energy PE [adapted from Sun et al., 1996].

Froude number $\delta_c = 1$ corresponds to the shear layer having the same horizontal kinetic energy HKE as the available potential energy APE of the stratification N while $\delta_c = 2$ (Miles, 1961; Howard, 1961) corresponds to the vorticity of the shear $|V_z|/2$ being able to overcome the stratification, $|V_z|/2 > N$. A $\delta_c = 1.7$ ($\mathrm{Ri}_c = 0.33 \pm 0.06$) has been cited (Thorpe, 1973) as the point when turbulence collapses. Laboratory data appear to support a critical $\delta_c = 2$ (Thorpe, 1971; Scotti and Corcos, 1972) but the geometry and history of the shear and stratification profiles appear to be important for δ_c and the form of the instability.

Ocean observations find no relation between gradient Froude number δ_N and turbulent dissipation rates ε unless δ_N is resolved on lengthscales small enough that unstable $\delta_N > \delta_c$ is resolved (Toole and Schmitt, 1987; Polzin, 1996). For typical ocean internal-wave fields, these require resolutions of 1–2 m.

Turbulent patch thicknesses L_P are often observed to be much thicker than both Ozmidov L_O and density overturn (Thorpe) L_T lengthscales (e.g., Gregg et al., 1986; Toole et al., 1997; Kunze et al., 2012). Thus, there are two potentially related spectral gaps between internal waves that generate turbulence and within the turbulence itself: (i) that between the spectral rolloff and the outer scales of turbulence (Fig. 1), and (ii) that between unstable shear-layer thicknesses and the outer scales of turbulence. Alternative explanations are that (i) the initial overturn scale is comparable to the patch thickness at the outset of instability but diminishes over the course of the turbulence patch's evolution as the turbulence decays (for example, see Wijesekera and Dillon, 1997; Smyth and Moum, 2000), and (ii) by analogy to surface-wave breaking, internal-wave breaking is associated with internal-wave packets or groups which set the patch dimensions (Thorpe, 2010).

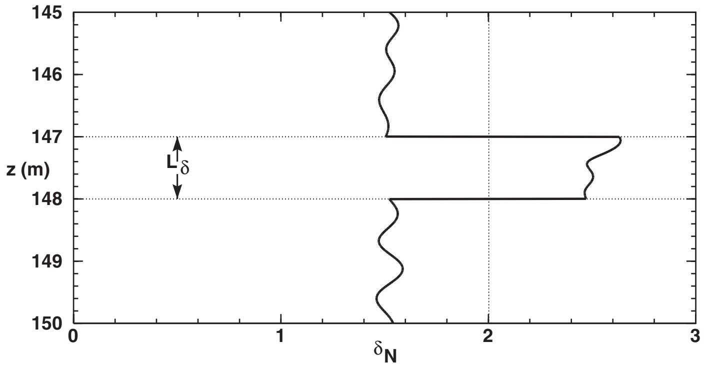

Figure 3. Cartoon showing a synthetic unstable ($\delta_c > 2$) shear layer of thickness $L_\delta = 1$ m between 147- and 148-m depth.

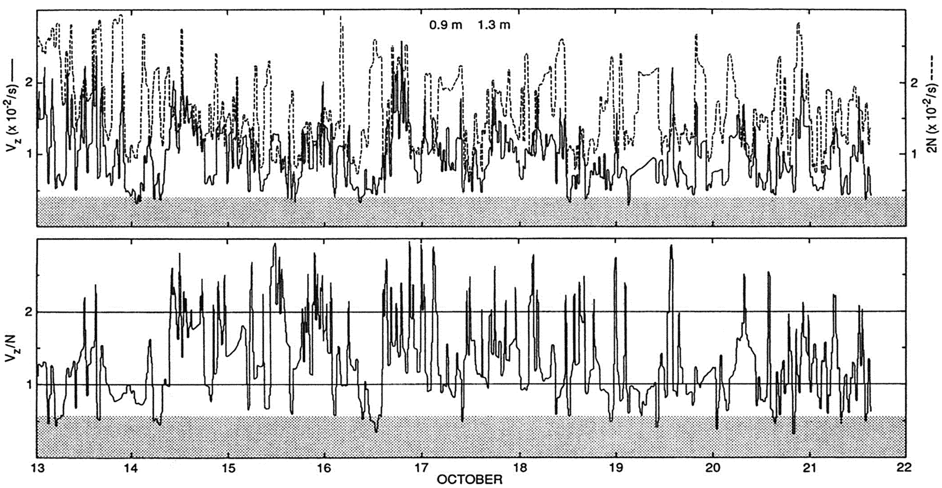

Figure 4. Nine-day time-series of 1-m shear magnitude $|V_z|$ (upper panel, solid line), buoyancy frequency N (upper panel, dashed line) and gradient Froude number $\delta_N = |V_z|/N$ (lower panel) from a neutrally-buoyant float deployed off the coast of California [adapted from Kunze et al., 1990].

Here, a more fundamental dynamical relationship is suggested based on the mechanism of shear instability at $|V_z| > \delta_c N$ (Miles, 1961; Howard, 1961) across an unstable shear layer of thickness L_δ (Fig. 3). Kunze et al. (1990) reported that for 1-m first-differences of velocity and density, $\delta_N \sim 1$ most of the time, jumping to values between 2 and 3 about 5% of the time (Fig. 4) and found no occurrences of $\delta_N > 2$ on vertical scales of 2-m. Polzin (1996) reported 0.28% of the total dissipation associated with 4-m $\delta_N > 2$ and 43% associated with 2-m $\delta_N > 2$; he also found 81% of the total dissipation associated with

4-m $\delta_N > 1$ and 88% associated with 2-m $\delta_N > 1$ He argued that gradient Froude number $\delta_N > 2$ occurs more frequently on smaller scales but cautioned that the lengthscale L_δ over which one chose to estimate δ_N must exceed the largest turbulence lengthscales L_O so that a fixed L_δ cannot be applied; in this sense, distinguishing unstable finescale shear from turbulence has similar issues to choosing an appropriate Thorpe density overturn scale so cannot be accomplished without high-resolution vertical profiles of both shear and stratification. Polzin (1996) argued that choosing L_δ such that $<V_z^2> > 1.0<N^2>$ allowed the parameterization to be used where the averaging $< \cdot >$ in space or time would be sufficient to produce a stable mean variance, typically 10–12 profiles or 10–12 buoyancy periods. An iterative approach to finding L_δ might also be effective.

3. Theory

A parameterization for the turbulence production rate $\varepsilon_p = 1.2\varepsilon$ was formulated by Kunze et al. (1990) which has been validated by fine- and microstructure ocean observations (Peters et al., 1995; Polzin, 1996). It depends on the available horizontal kinetic energy (HKE) in an unstable shear layer of thickness L_δ, $(V_z^2 - \delta_c^2 N^2)L_\delta^2/24 = N^2 L_\delta^2(\delta_N^2 - \delta_c^2)/24$ (Thomson, 1980) and the Kelvin-Helmholtz growth rate $\sigma = (|V_z| - \delta_c N)/4 = (\delta_N - \delta_c)N/4$ (Hazel, 1972). Note that there is zero available HKE and zero growth rate σ at critical gradient Froude number $\delta_N = \delta_c$. The growth rate σ does not exceed N until $\delta_N > 4 + \delta_c$.

The turbulence production rate ε_p can then be expressed in terms of the gradient Froude number $\delta_N = |V_z|/N = \mathrm{Ri}^{-1/2}$

$$\varepsilon_p = (1+\gamma)\varepsilon = L_\delta^2 N^3 \frac{\left(\delta_N^2 - \delta_c^2\right)(\delta_N - \delta_c)}{96} H(\delta_N - \delta_c) \tag{1}$$

(Kunze et al., 1990) where L_δ is the thickness of the unstable ($\delta_N > \delta_c$) shear layer which is assumed to break down into turbulence, and $H(\cdot)$ is the Heaviside function. Likewise, the patch-average dissipation rate $<\varepsilon>$ has been expressed in terms of the Ozmidov (1965) or overturning (Thorpe, 1977) lengthscales

$$\varepsilon = L_O^2 N^3 = 0.64 L_T^2 N^3. \tag{2}$$

Equating (1) and (2) for dissipation rate ε, the ratio of the Ozmidov lengthscale to unstable shear-layer thickness is

$$\frac{L_O}{L_\delta} = \frac{(\delta_N - \delta_c)\sqrt{\delta_N + \delta_c}}{4\sqrt{6}}. \tag{3}$$

For a critical Froude number $\delta_c = 2$ (Fig. 5), the ratio is less than 1 for $2 < \delta_N < 5.5$ [corresponding to $0.03 < \mathrm{Ri} < 0.25$] and greater than 1 for $\delta_N > 5.5$; choosing $\delta_c = 1$, leads to a ratio less than 1 for $1 < \delta_N < 5$ and greater than 1 for $\delta_N > 5$. Thus, the existence of a spectral gap between the smallest internal-wave (L_δ) and largest turbulent (L_O, L_T) lengthscales is predicted to be a function of how unstable the shear layer is. For moderately

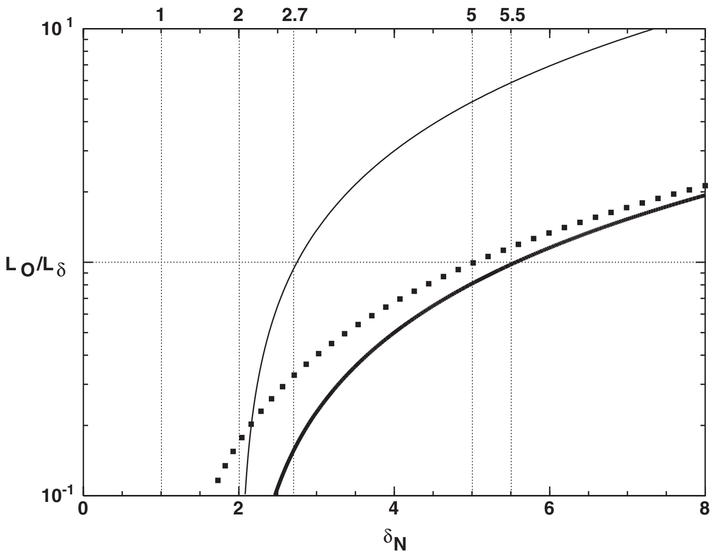

Figure 5. Lengthscale ratio L_O/L_δ as a function of gradient Froude number δ_N (3) for critical gradient Froude number $\delta_c = 2$ (thick solid) and 1 (dotted) where $L_O = (\varepsilon/N^3)^{1/2}$ is the Ozmidov lengthscale and L_δ the thickness of the unstable ($\delta_N > \delta_c$) shear layer. The ratio lies below one for $\delta_N < 5.5$ [corresponding to Ri < 0.03] with $\delta_c = 2$ (thick solid curve) so that turbulent overturn scales will be smaller than the patch thickness $L_P (= L_\delta)$, and above one for $\delta_N > 5.5$ so that the unstable shear layer will entrain water from the neighboring fluid; for $\delta_c = 1$, the ratio transition occurs for $\delta_N = 5$ (dotted curve). The turbulent patch thickness L_P is expected to scale to the larger of L_O and L_δ. Taking into account that an overturn spanning L, which might be a more appropriate measure of patch thickness, has an rms $L_T = L/6$, yields the thin solid curve for which the patch thickness is only thicker than the overturn length for $\delta_N < 2.7$.

unstable gradient Froude number, overturns L_O are smaller than the unstable shear layer thickness L_δ. If a turbulence patch thickness L_P corresponds to the unstable shear layer thickness $L_\delta (L_P = L_\delta)$, then we also expect $L_O < L_P$. Gregg et al. (1986) reported patch thicknesses of 0.5–8 m and Ozmidov scales O(0.1 m) consistent with lengthscale ratios of 0.02–0.1, and implying $\delta_N < 3$ responsible for their patches if the arguments leading to (3) hold. For higher gradient Froude numbers ($\delta_N > 5.5$), predicted overturn lengthscales are larger than the shear layer thickness and turbulence is expected to entrain water from outside the unstable shear layer as has been reported in some lab experiments.

Note that other parameterizations also predict a spectral gap in vertical wavenumber k_z space between internal waves (L_r, L_δ) and turbulence (L_O, L_T) (Fig. 1). Equating the internal-wave cascade parameterization for turbulent dissipation rate

$$\varepsilon = \varepsilon_0 \frac{N^2}{N_0^2} \frac{E^2}{E_{\mathrm{GM}}^2} h(R_\omega) j\left(\frac{f}{N}\right) = \varepsilon_0 \frac{N^2}{N_0^2} \frac{L_r^2}{L_{\mathrm{GM}}^2} h(R_\omega) j\left(\frac{f}{N}\right) \tag{4}$$

(Henyey et al., 1986; Gregg, 1989; Polzin et al., 1995; Gregg et al., 2003) where $\varepsilon_0 = 7 \times 10^{-10}$ W kg^{-1}, $N_0 = 5.3 \times 10^{-3}$ rad s^{-1}, R_ω is the shear/strain variance ratio and $L_{GM} = 10$ m/(2π), to the Ozmidov lengthscale relation (2),

$$\frac{L_O^2}{L_r^2} = \frac{4\pi^2\varepsilon_0}{N_0^2 N L_{GM}^2} f(R_\omega) j\left(\frac{f}{N}\right) \tag{5}$$

with variability only due to buoyancy frequency N, the shear/strain variance ratio R_ω and latitude (f). As pointed out by D'Asaro and Lien (2000), the two lengthscales both depend on E^2 so will parallel each other as the internal-wave field rises and falls. For an oceanic shear/strain variance ratio $R_\omega = 7$, $f(R_\omega) = 0.5$. For $N = 10^{-4} - 10^{-1}$ rad s^{-1} and $f = 0 - 10^{-4}$ rad s^{-1}, the lengthscale ratio $L_O/L_r < 0.06$. Thus, (5) also predicts a large spectral gap between the largest turbulence and smallest internal-wave lengthscales, consistent with ocean observations (Fig. 1). It predicts that the gap will be wider for higher N near the equator and narrower for lower N at high latitudes.

4. Summary

For a critical gradient Froude number $\delta_c = 2$, unless the gradient Froude number δ_N exceeds 5.5, the Ozmidov L_O and overturning L_T turbulent lengthscales will be smaller than the unstable-shear-layer thickness L_δ (Fig. 5) or, equivalently, overturning scales will be smaller than turbulent patch thicknesses L_P, as often observed (Gregg et al., 1986; Toole et al., 1997; Kunze et al., 2012). This satisfies the assumption of scale separation between fine- and microscales for a Reynolds decomposition, and is consistent with the shear spectrum (Fig. 1).

In the case where $\delta_N > 5.5$ (Ri < 0.03), Ozmidov and overturn lengthscales are predicted to be larger than the unstable layer so turbulence should entrain water from outside the unstable shear layer and the patch thickness L_P will grow. In this case, there would be no scale separation between outer turbulence and the finescale internal-wave shear that generates it. Thus, scale separation between internal waves and turbulence is predicted to depend on whether unstable shear layer in the ocean are moderately ($\delta_N < 5.5$; Ri > 0.03) or strongly unstable.

We caution that other explanations are possible as already mentioned. As pointed out by Thorpe (2010), for an overturn spanning a thickness L, the rms $L_T \sim L/6$ and it is this rms L_T that is comparable to L_O on average. Taking this into account, patch thicknesses only exceed L for $\delta_N < 2.7$ (thin solid curve in Fig. 3). Stratified turbulent boundary layers are often 1–2 orders of magnitude thicker than overturning or Ozmidov scales (Toole et al., 1997; Kunze et al., 2012), much thicker than one would expect from the explanation offered here. These likely arise from multiple superposed and overlapping unstable shear layers being strongly forced by boundary processes such as near-critical internal wave reflection. Even in the interior, the passage of wave groups may create turbulence patches thicker than overturning scales (Thorpe 2010). Thus, the explanation offered here is only one of many.

Acknowledgments. This note was provoked by J. Nash's skepticism that unstable shear layer thickness L_δ in (1) had any physical significance. Valuable comments were supplied by Ken Brink, Steve Thorpe, and an anonymous reviewer.

REFERENCES

D'Asaro, E. A., K. B. Winters, and R.-C. Lien. 2004. Lagrangian estimates of diapycnal mixing in a simulated K-H instability. J. Atmos. Oceanic Technol., *21*, 799–809.

D'Asaro, E. A., and R.-C. Lien. 2000. The wave-turbulence transition for stratified flows. J. Phys. Oceanogr., *30*, 1669–1678.

Dillon, T. M. 1982. Vertical overturns: A comparison of Thorpe and Ozmidov lengthscales. J. Geophys. Res., *87*, 9601–9613.

Dillon, T. M., and M. M. Park. 1987. The available potential energy of overturns as indicator of mixing in the seasonal thermocline. J. Geophys. Res., *92*, 5345–5353.

Eckermann, S. D. 1999. Isentropic advection by internal waves: Quasi-universal m^{-3} vertical wavenumber spectra near the onset of instability. Geophys. Res. Lett., *26*, 201–204.

Fritts, D. C. 1984. Gravity wave saturation in the middle atmosphere: A review of theory and observations. Rev. Geophys., *22*, 275–308.

Gargett, A. E., P. J. Hendricks, T. B. Sanford, T. R. Osborn, and A. J. Williams III. 1981. A composite spectrum of vertical shear in the ocean. J. Phys. Oceanogr., *11*, 1258–1271.

Gargett, A. E., T. R. Osborn, and P. W. Nasmyth. 1984. Local isotropy and the decay of turbulence in a stratified fluid. J. Fluid Mech., *144*, 231–280.

Gregg, M. C., E. A. D'Asaro, T. J. Shay, and N. Larson. 1986. Observations of persistent mixing and near-inertial internal waves. J. Phys. Oceanogr., *16*, 856–885.

Gregg, M. C., and T. B. Sanford. 1988. The dependence of turbulent dissipation on stratification in a diffusively-stable thermocline. J. Geophys. Res., *93*, 12,381–12,392.

Gregg, M. C. 1989. Scaling turbulent dissipation in the thermocline. J. Geophys. Res., *94*, 9686–9698.

Gregg, M. C., and E. Kunze. 1991. Internal wave shear and strain in Santa Monica basin. J. Geophys. Res., *96*, 16,709–16,719.

Gregg, M. C., D. P. Winkel and T. B. Sanford. 1993. Fully resolved spectra of vertical shear. J. Phys. Oceanogr., *23*, 124–141.

Gregg, M. C., T. B. Sanford, and D. P. Winkel. 2003. Reduced mixing from the breaking of internal waves in equatorial ocean waters. Nature, *422*, 513–515.

Hazel, P. 1972. Numerical studies of the stability of inviscid stratified shear flows. J. Fluid Mech., *51*, 39–61.

Henyey, F. S., J. Wright and S. M. Flatte. 1986. Energy and action flow through the internal wave field: An eikonal approach. J. Geophys. Res., *91*, 8487–8495.

Hines, C. O. 1993. The saturation of gravity waves in the middle atmosphere. Part 4: Cutoff of the incident wave spectrum. J. Atmos. Sci., *50*, 3045–3060.

Hines, C. O. 1996. Nonlinearity of saturated-gravity-wave spectra in the middle atmosphere. Geophys. Res. Lett., *23*, 3309–3312.

Howard, L. N. 1961. Note on a paper of John W. Miles. J. Fluid Mech., *10*, 509–512.

Kunze, E., A. J. Williams III, and M. G. Briscoe. 1990. Observations of shear and vertical stability from a neutrally-buoyant float (Part 1). J. Geophys. Res., *95*, 18, 127–18, 142.

Kunze, E., C. MacKay, E. E. McPhee-Shaw, K. Morrice, J. B. Girton, and S. R. Terker. 2012. Turbulent mixing and exchange with interior waters on sloping boundaries. J. Phys. Oceanogr., *42*, 910–927.

Lelong, M.-P., M. A. Sundermeyer and E. Kunze. 2002. Numerical simulations of lateral dispersion by the relaxation of diapycnal mixing events. EOS Transac., *83*(*Suppl.*), 227.
Miles, J. W. 1961. On the stability of heterogeneous shear flows. J. Fluid Mech., *10*, 496–508.
Munk, W. 1981. Internal waves and small scale processes, *in* Evolution of Physical Oceanography, B. A. Warren and C. A. Wunsch, eds. Cambridge: The MIT Press, 623 pp.
Ozmidov, R. V. 1965. On the turbulent exchange in a stably stratified ocean. Izv. Acad. Sci. USSR Atmos. Oceanic Phys., English Transl., *1*, 853–860.
Peters, H., M. C. Gregg, and T. B. Sanford. 1995. On the parameterization of equatorial turbulence: Effect of finescale variations below the range of the diurnal cycle. J. Geophys. Res., *100*, 18,333–18,248.
Polzin, K. L., J. M. Toole, and R. W. Schmitt. 1995. Finescale parameterizations of turbulent dissipation. J. Phys. Oceanogr., *25*, 306–328.
Polzin, K. L. 1996. Statistics of the Richardson number: Mixing models and finestructure. J. Phys. Oceanogr., *26*, 1409–1425.
Polzin, K. L., E. Kunze, J. M. Toole and R. W. Schmitt. 2003. The partition of finescale energy into internal waves and geostrophic motions. J. Phys. Oceanogr., *33*, 234–248.
Richardson, L. F. 1920. The supply of energy form and to atmospheric eddies. Proc. Roy. Soc. Lond. A, *97*, 354–373.
Scotti, R. S., and G. M. Corcos. 1972. An experiment on the stability of small disturbances in a stratified free-shear layer. J. Fluid Mech., *52*, 499–528.
Smith, S. A., D. C. Fritts, and T. E. Van Zandt. 1987. Evidence of a saturated spectrum of atmospheric gravity waves. J. Atmos. Sci., *44*, 1404–1410.
Smyth, W. D., and J. N. Moum. 2000. Lengthscales of turbulence in stably-stratified mixing layers. Phys. Fluids, *12*, 1327–1342.
Sun, H., E. Kunze, and A. J. Williams III. 1996. Vertical heat-flux measurements from a neutrally-buoyant float. J. Phys. Oceanogr., *26*, 984–1001.
Sundermeyer, M. A., and M.-P. Lelong. 2005. Numerical simulations of lateral dispersion by the relaxation of diapycnal mixing events. *J. Phys. Oceanogr.*, 35, 2368–2386.
Thomson, R. O. R. Y. 1980. Efficiency of conversion of kinetic energy and potential energy by breaking internal waves. J. Geophys. Res., *85*, 6631–6635.
Thorpe, S. A. 1971. Experiments on the instability of stratified shear flows: Miscible flows. J. Fluid Mech., *46*, 299–319.
Thorpe, S. A. 1973. Experiments on instability and turbulence in a stratified shear flow. J. Fluid Mech., *61*, 731–751.
Thorpe, S. A. 1977. Turbulence and mixing in a Scottish loch. Philos. Trans. Roy. Soc. Lond. A, *286*, 125–181.
Thorpe, S. A., 2010. Breaking internal waves and turbulent dissipation. J. Mar. Res., *68*, 851–880.
Toole, J. M., and R. W. Schmitt. 1987. Smallscale structures in the northwest Atlantic subtropical front. Nature, *327*, 47–49.
Toole, J. M., R. W. Schmitt, K. L. Polzin, and E. Kunze. 1997. Near-boundary mixing above the flanks of a mid-latitude seamount. J. Geophys. Res., *102*, 947–959.
Wijesekera, H. W., and T. M. Dillon. 1997. Shannon entropy as an indicator of age for turbulent overturns in the oceanic thermocline. J. Geophys. Res., *102*, 3279–3291.

Received: *1 March 2014*; revised: *21 June 2014*.